Journal of Structural Geology 105 (2017) 80–87

Contents lists available at ScienceDirect

Journal of Structural Geology

journal homepage: www.elsevier.com/locate/jsg

# Stress dependence of microstructures in experimentally deformed calcite

John P. Platt[a,*], J.H.P. De Bresser[b]

[a] Department of Earth Sciences, University of Southern California, Los Angeles, CA, 90089-0742, USA
[b] HPT-laboratory, Department of Earth Sciences, PO Box 80.021, 3508 TA, Utrecht University, The Netherlands

ARTICLE INFO

*Keywords:*
Dynamically recrystallized grain-size
Subgrain
Grain-boundary migration
Lattice strain energy
Grain-boundary energy

ABSTRACT

Optical measurements of microstructural features in experimentally deformed Carrara marble help define their dependence on stress. These features include dynamically recrystallized grain size (*Dr*), subgrain size (*Sg*), minimum bulge size ($L\rho$), and the maximum scale length for surface-energy driven grain-boundary migration ($L\gamma$). Taken together with previously published data *Dr* defines a paleopiezometer over the range 15–291 MPa and temperature over the range 500–1000 °C, with a stress exponent of −1.09 (CI −1.27 to −0.95), showing no detectable dependence on temperature. *Sg* and *Dr* measured in the same samples are closely similar in size, suggesting that the new grains did not grow significantly after nucleation. $L\rho$ and $L\gamma$ measured on each sample define a relationship to stress with an exponent of approximately −1.6, which helps define the boundary between a region of dominant strain-energy-driven grain-boundary migration at high stress, from a region of dominant surface-energy-driven grain-boundary migration at low stress.

## 1. Introduction

Plastic deformation of crystalline solids produces distinctive and informative microstructures (e.g., White, 1976). These include lattice distortion, which reflects the density of lattice defects; low-angle tilt and twist boundaries within grains, which reflect the operation of recovery processes such as dislocation climb; and dynamic recrystallization, which reflects a variety of processes that produce new grains as well as the migration of grain-boundaries driven by lattice strain energy and grain-boundary surface energy (Karato, 1988; Hirth and Tullis, 1992). Features such as the crystallographic preferred orientation, dynamically recrystallized grain size, subgrain size, twin density, and dislocation density can provide a wealth of information, both about the slip systems active during deformation (Lloyd et al., 1997; Halfpenny et al., 2006), and on the physical conditions during deformation. Experimental deformation under controlled conditions can provide calibrations of the relationships between microstructural features and deformational parameters including temperature (e.g., Barnhoorn et al., 2004; ter Heege et al., 2005), water content (e.g., Jung and Karato, 2001; Stipp and Tullis, 2006), and differential stress (e.g. Karato et al., 1980; van der Wal et al., 1993; Post and Tullis, 1999; Stipp and Tullis, 2003; Siemes et al., 2011; Kidder et al., 2016; Cross et al., 2017).

A substantial amount of experimental work has been done on calcite marble from the Carrara quarries in the northern Italian Apennines, because of its purity, homogeneity, and lack of significant shape or crystallographic fabric (Schmid et al., 1980; Rutter, 1995; Pieri et al., 2001a, 2001b; ter Heege et al., 2002; Barnhoorn et al., 2004; De Bresser et al., 2005), and these experiments have provided information on the rheological properties, deformational mechanisms, and microstructural processes of calcite in general and Carrara marble in particular. Deformed samples from a series of experiments carried out at Utrecht University, the Netherlands (ter Heege et al., 2002; De Bresser et al., 2005) and ANU Canberra, Australia (De Bresser et al., 2005) were archived, and some were subsequently studied in detail by Valcke et al. (2006, 2007, 2014) who documented microstructural relationships among deformed grains, dynamically recrystallized grains, subgrains, and grain-boundary bulges. This paper builds on these studies, with the specific aim of testing recently developed hypotheses about dynamic recrystallization, nucleation, and grain-size evolution (De Bresser et al., 1998; Shimizu, 1998; De Bresser et al., 2001; Kellermann Slotemaker and De Bresser, 2006; Austin and Evans, 2007, 2009; Platt and Behr, 2011; Herwegh et al., 2014).

A particular goal of this work was to locate the boundary in stress/grain-size space between the regions where lattice strain energy and surface energy respectively provide the dominant driver for grain-boundary migration. These two regions should show significantly different microstructures, and grain growth is only likely to occur in the region where surface energy dominates (Platt and Behr, 2011). This line, known as the $D_{min}$ line, is predicted on theoretical grounds to be temperature independent, with a slope of 2 in log stress/log grain-size space, but as far as we know it has not been confidently located for any material.

* Corresponding author.
*E-mail address:* jplatt@usc.edu (J.P. Platt).

https://doi.org/10.1016/j.jsg.2017.10.012
Received 27 June 2017; Received in revised form 29 October 2017; Accepted 30 October 2017

**Table 1**
Experimental and microstructural data. ln(e), natural strain. Stress is differential stress at the end of the experiment, except for 36LM900 (starred), for which it is the average of the stresses measured at the end of the first three of four strain steps. *Dr*, dynamically recrystallized grain size (RMS of equivalent circle diameter). *Sg*, subgrain size, measured in the same way as *Dr*. *Lρ*, minimum diameter of viable bulges. *Lγ*, maximum scale length of surface-energy driven grain-boundary migration. Samples coded LM from ter Heege et al. (2002), the other samples from De Bresser et al. (2005). See text for further explanation.

| Sample # | % axial shortening | ln(e) | T°C | stress MPa | *Dr μm* | ± *Dr* (*n*) | *Sg μm* | ± *Sg* (*n*) | *Lρ* | *Lγ* |
|---|---|---|---|---|---|---|---|---|---|---|
| 15LM950 | 36 | −0.45 | 962 | 14.6 | 79 | 23 (72) | 72 | 21 (50) | 46 | 58 |
| 25LM950 | 36 | −0.45 | 950 | 24.8 | 31.6 | 12 (39) | 23.9 | 15 (36) | 12 | 10 |
| 23LM900 | 36 | −0.45 | 900 | 21.8 | 43 | 13 (33) | 35 | 13 (19) | 10.8 | 11 |
| 36LM900 | 59 | −0.9 | 900 | 34.4* | 13.9 | 5 (41) | 13.9 | 5 (26) | 7 | 9 |
| 50LM900 | 36 | −0.45 | 900 | 44.4 | 36 | 13 (47) | 37 | 11 (7) | 7 | 11 |
| 50LM780 | 36 | −0.45 | 780 | 47.3 | 13.5 | 7 (25) | 13.1 | 5 (27) | 3 | 4 |
| 50LM730 | 36 | −0.45 | 730 | 52.1 | 13.8 | 2 (30) | 11 | 3 (22) | 4.5 | 7 |
| 65LM700 | 36 | −0.45 | 700 | 65.0 | 14.1 | 2 (49) | 10.5 | 3 (29) | 4 | 6 |
| 85LM730 | 36 | −0.45 | 730 | 82.1 | | | 5.2 | 2 (13) | 2 | |
| 5347 | 21 | −0.24 | 1000 | 27.5 | 41 | 14 (29) | 43 | 25 (15) | 16 | 13 |
| 5356 | 21 | −0.24 | 1000 | 21.6 | 34 | 12 (71) | 30 | 13 (11) | 13 | 13 |
| 5348 | 20 | −0.22 | 800 | 63.9 | 22 | 9 (39) | 22 | 11 (39) | 6.6 | 7.3 |
| 5321 | 10 | −0.11 | 800 | 45.8 | 33 | 15 (33) | 30 | 15 | 8 | 10 |
| 5325 | 13 | −0.14 | 800 | 44.5 | 25 | 10 (50) | 32 | 15 | 8 | 9 |
| 5332 | 26 | −0.30 | 800 | 71.4 | 20 | 7 (35) | 22 | 11 | 3 | 4.5 |

## 2. Methods

The original experiments were carried out in axial compression by constant displacement rate tests in a constant volume, internally heated argon gas-medium apparatus (Utrecht University or ANU Canberra) under a confining pressure of 300 MPa to natural strains of 0.15–0.90 at strain rates of $3 \times 10^{-6}$ to $4.9 \times 10^{-4}$ $s^{-1}$ and temperatures of 700–1000 °C (ter Heege et al., 2002; De Bresser et al., 2005). The samples were rapidly quenched after deformation to preserve the microstructures. Differential stresses during the experiments ranged from 15 to 90 MPa. In most experiments stress reached a peak at a natural strain of 0.02–0.1, and then progressively dropped by up to 12 MPa during deformation. As discussed later, for all but one of the experiments we have used the final stress when assessing the significance of the microstructures. Temperature and stress during deformation for the samples we analyzed are shown in Table 1.

Electron backscatter diffraction analysis (EBSD) on the scanning electron microscope is increasingly used as the technique of choice for microstructural analysis of deformed mineral aggregates (e.g., Prior et al., 1999, 2009), and was the basis for the studies of Valcke et al. (2006, 2007 and 2014). EBSD has several clear advantages; it provides higher resolution than optical studies; it allows grains and subgrains to be distinguished precisely in terms of their complete crystallographic orientation and their lattice misorientation with respect to their neighbours; and it provides maps that can be rapidly analyzed in terms of grain size and grain shape.

Other techniques that may be appropriate in particular situations include traditional optical microscopy and etching of polished surfaces. A distinctive feature of calcite is that its high birefringence means that thin-sections as little as 5 μm thick show first-order interference colours under the optical microscope, which allows optical study of features at scales that are only limited by the wavelength of light (~0.5 μm). The sharp relief contrast on grain boundaries allows features such as grain-boundary bulges to be imaged very precisely, and the ability of the microscope to focus through the thickness of the section means that the 3-D geometry of such features can be characterized effectively. As discussed below, two of the principle aims of this study were to measure the minimum size of grain-boundary bulges *Lρ*, and the scale length *Lγ* of grain-boundaries that have been modified by surface-energy-driven grain boundary migration (referred to here as γ-GBM, after Platt and Behr, 2011) (Fig. 1). Both these features are difficult to identify and measure with EBSD unless very small step sizes are used, which places practical limits on the area that can be examined in detail. Optical microscopy allows large areas to be scanned rapidly for pertinent microstructures, which can then be studied at high resolution. For these reasons, this study was carried out on using optical microscopy on ultra-thin sections.

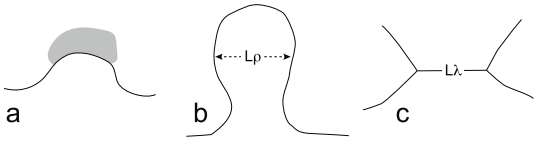


**Fig. 1.** a) Sketch of a grain boundary bulge that has not amplified much. This may be transient, driven by a local region of high dislocation density, and hence liable to shrinkage and elimination driven by γ-GBM. b) Sketch of a grain-boundary bulge that has amplified to the point that its length is greater than its diameter. This is likely to indicate that amplification is driven by the ambient average dislocation density, and hence that the bulge is likely to survive. The minimum size of such bulges defines the scale length *Lρ* of ρ-GBM. c) Sketch of a straight grain-boundary bounded by ~120° triple junctions. The length of the grain-boundary defines the scale length of γ-GBM.

A challenging aspect of studying the process of dynamic recrystallization in experimentally deformed samples that have only reached low strains, and hence low proportions of new grains, is distinguishing new grains from the remnants of the original grains, which may be dissected by kink-bands, twins, fractures, or micro-scale shear zones. The study by Valcke et al. (2014), for example, placed particular importance on the use of EBSD for the identification of recrystallized grains based on their lack of substructure (lattice distortion and subgrains), which provides a systematic and objective criterion for microstructural description. A potential problem with this approach is that in a deforming medium, some new grains may have a significant dislocation density, and hence may show lattice distortion and small-scale dislocation cells or subgrains. One reason for this is that new grains formed by the subgrain rotation mechanism (SGR) are likely to have a dislocation density, and hence lattice misorientation, comparable to their parent grains. Also, new grains formed by the grain-boundary bulging mechanism (BLG) may have low dislocation densities initially, but this makes them relatively soft, so they deform more rapidly than the bulk aggregate, and their dislocation density increases rapidly after nucleation (Humphreys and Hatherly, 2004). The net result is that many recrystallized grains are likely to be overlooked, with unpredictable effects on the resulting grain-size distribution.

Optical microscopy allows an alternative approach to the definition of recrystallized grains that may lead to somewhat different results and insights. New grains can be identified based on a number of microstructural criteria that can be rapidly determined by inspection under the optical microscope. In many samples, recrystallized grains form aggregates of sub-equant grains that are distinctly smaller than relict primary grains, and have more regular shapes than dissected remnants